Journal of Integrative Agriculture 2026, 25(2): 610–623

Available online at ScienceDirect

Journal of Integrative Agriculture



RESEARCH ARTICLE

Unbalanced lipid metabolism in anther, especially the disorder of the alpha-linolenic acid metabolism pathway, leads to cotton male sterility

Lihong Ma[1], Pengtao Wang[2], Qian-Hao Zhu[3], Xinqi Cheng[4], Tao Zhang[1], Xinyu Zhang[1], Huaguo Zhu[4], Zuoren Yang[5], Jie Sun[1#], Feng Liu[1#]

[1] *Key Laboratory of Oasis Eco-agriculture, College of Agriculture, Shihezi University, Shihezi 832000, China*
[2] *State Key Laboratory of Crop Stress Adaptation and Improvement/College of Life Sciences, Henan University, Kaifeng 475000, China*
[3] *CSIRO Agriculture and Food, GPO Box 1700, Canberra 2601, Australia*
[4] *College of Biology and Agricultural Resources, Huanggang Normal University, Huanggang 438000, China*
[5] *State Key Laboratory of Cotton Biology/Institute of Cotton Research, Chinese Academy of Agricultural Sciences, Anyang 455000, China*

Highlights

- Imbalanced lipid profiles in male sterile cotton anthers, featuring over-accumulation of free fatty acids (FFAs), phosphatidic acid (PA), mono-galactosyldiacylglycerol (MGDG), and di-galactosyldiacylglycerol (DGDG), alongside reduced triacylglycerol (TAG), disrupt normal pollen development.
- alpha-Linolenic acid (C18:3) metabolism disruption is central to sterility, with excess MGDG/DGDG elevating jasmonic acid (JA) levels, which feedback-inhibits *GhFAD3* and further reduces C18:3.
- CRISPR/Cas9 knockout of *GhFAD3* confirms its essential role in anther development, as mutants show no pollen, reduced TAG/C18:3, and male sterility.

Abstract

Recent studies have shown that lipid metabolism is a key factor affecting anther development and male fertility. However, how plants regulating the metabolic balance of multiple lipids to ensure proper anther development and male fertility remains unclear. Analyzing lipid molecules related to anther fertility and genes responsible for their biosynthesis is crucial for understanding the physiological significance of lipid metabolism in crop fertility. In this study, we compared the transcriptome and the composition and content of lipids in anthers of two upland cotton (*Gossypium hirsutum*) materials, Shida 98 (WT) and its nearly-isogenic male sterile line Shida 98A (MS). Transcriptomics analysis identified many differentially expressed genes (DEGs) between the two materials, with the genes of the alpha-linolenic acid metabolism pathway being the most significantly associated with the male sterility phenotype. Investigations on lipids revealed that the MS anthers over-accumulated free fatty acids (FFAs), phosphatidic acid (PA), mono- and di-galactosyldiacylglycerol (MGDG and DGDG), and had a decreased content of triacylglycerol (TAG), which was closely related to the abnormal metabolism of alpha-linolenic acid (C18:3); therefore, the major lipids containing C18:3-acyl chains, such as PA, MGDG, DGDG, and TAG, are proposed to play a major role in cotton anther development. We also showed that an excessive level of MGDG and DGDG caused jasmonic acid (JA) overaccumulation in MS anthers, which in turn inhibited the expression of *GhFAD3* and consequently reduced the C18:3 content, presumably *via* a feedback regulation mechanism, ultimately affecting plant fertility. Together, our results revealed the importance of a balanced lipid metabolism in regulating the development of cotton anther and pollen and consequently male fertility.

Keywords: cotton, anther, male sterility, lipid metabolism, alpha-linolenic acid

1. Introduction

Male sterility (MS) is an effective pollination control system and an important tool for hybrid seed production. Understanding the development of anther is essential

Received 25 April 2024; Received in revised form 7 June 2024; Accepted 13 June 2024; Available online 22 July 2024
#Correspondence Jie Sun, E-mail: sunjie@shzu.edu.cn; Feng Liu, E-mail: liufeng@shzu.edu.cn

© 2026 CAAS. Publishing services by Elsevier B.V. on behalf of KeAi Communications Co. Ltd. This is an open access article under the CC BY-NC-ND license (http://creativecommons.org/licenses/by-nc-nd/4.0/). Peer review under responsibility of Editorial Board of *Journal of Integrative Agriculture*.
doi: 10.1016/j.jia.2024.07.036

for sexual reproduction. Many studies have probed physiological and biochemical changes during anther development in different plant species (Sawhney and Shukla 1994; Jiang *et al.* 2007; Pressman e*t al.* 2012; Zhu *et al.* 2022). Lipids, as structural components, energy supplies, and signal transduction molecules, play crucial roles in male reproductive development of flowering plants (Wan e*t al.* 2020). In both the endoplasmic reticulum (ER) and plastid, phosphatidic acid (PA) is the first lipid species formed by *de novo* complete acylation of glycerol-3-phosphate (G-3-P) (Lavell and Benning 2019), and is the precursor of other phospholipids and the second messenger of lipids (Zegarlińska *et al.* 2018). PA can be converted to diacylglycerol (DAG) by PA phosphatase or to cytidine diphosphate diacylglycerol (CDP-DAG) by CDP-DAG synthase to further form phosphatidylinositol (PI) and phosphatidylglycerol (PG) (Vance and Vance 2004; Han and Carman 2010). DAG can also be synthesized into membrane lipids or directly into storage lipid triacylglycerol (TAG) (Li-Beisson *et al.* 2013; Bates 2016; Maraschin *et al.* 2019). In eukaryotes, phosphatidylcholine (PC) is the vector for desaturation of fatty acids (FAs). Subsequently, FAs are incorporated into TAG and packaged in lipid droplets (or oil bodies) as carbon and energy reserve (He and Ding 2020). The mono- and di-galactosyldiacylglycerol (MGDG and DGDG) are the main lipids in chloroplast membrane, collectively referred to as galactolipids, they are closely related to photosynthetic properties (Block *et al.* 1983; Benning 2009; Yu *et al.* 2020). While lipid metabolism has been a hot research topic in elucidating the mechanisms underlying male fertility of plants (Wan *et al.* 2020), a holistic understanding of plant lipid metabolism and its association with male fertility is still lacking thanks to its complexity.

Cotton is one of the important industrial crops. Unlike *Arabidopsis* and rice, cultivated cotton is an allotetraploid with complex genome (AADD, 2n=4×=52). Due to the lack of suitable male sterile materials to produce F_1 seeds and the high cost of manually producing F_1 seeds, utilization of heterosis is limited in cotton production. Understanding the molecular genetic mechanism of cotton male sterility is of great significance for the utilization of cotton heterosis. A recent study has shown that mutations in *GhCYP703A2*, which catalyzes the hydroxylation of fatty acids, lead to male sterility, which has been successfully used to develop hybrid cotton lines (Ma *et al.* 2022). And how plants regulate metabolic balance of multiple lipids to promote normal anther development remains elusive.

In this study, we conducted phenotypic and physiological observations on cotton variety Shida 98 (WT) and its nearly-isogenic male sterile line Shida 98A (MS), and investigated the impact of lipid metabolism in MS anthers. Comparative transcriptome analysis between WT and MS revealed significant changes in many lipid related pathways in MS anthers. A comprehensive molecular network was created by combining lipomic and transcriptomic data and fatty acid composition, showing changes in major lipid metabolites and genes associated with male sterility in cotton anthers. Our study revealed that the excessive accumulation of FFAs, PA, MGDG, and DGDG, as well as the lack of TAG, in anthers impaired cotton male fertility, and proper alpha-linolenic acid metabolism and a functional *GhFAD3* are crucial for cotton anther development and male fertility. This is the first systematic study on lipid metabolism and its regulatory network in cotton anthers. The results are of great significance for in-depth understanding of the molecular and physiological significance of lipid metabolism in anther development.

2. Materials and methods

2.1. Plant materials

Upland cotton materials were Shida 98 (WT) and its nearly-isogenic male sterile line Shida 98A (MS), which were provided by the Cotton Research Institute of Shihezi University in Xinjiang, China. Cotton materials were grown in the experimental field of the Cotton Institute of Shihezi University. Anthers of four developmental stages, i.e., meiosis (M), tetrad (T), mononuclear and binuclear pollen (MB), and pollen maturation (PM) stages, were collected from MS and WT plants according to Cheng *et al.* (2020).

2.2. Phenotypic analysis and cytological analysis

Anthers and flowers of MS and WT were photographed with a digital camera (Canon, Japan). To test pollen viability, pollen grains were stained with two to three drops of Alexander's solution or I_2-KI solution, and then photographed using a SteREO Discovery microscope (Carl Zeiss, Germany). For scanning electron microscopy observation, anthers of WT and MS at the pollen maturation stage were fixed overnight in 2.5% glutaraldehyde, and then washed and postfixed with 1% osmium tetraoxide in 0.1 mol L^{-1} sodium phosphate buffer (PBS, pH 7.2). Finally, samples were visualized using the method described by Liu *et al.* (2019).

2.3. Transcriptome analysis

Anthers collected at different stages were sent to Novogene Bioinformatics Technology (Beijing, China) for RNA extraction and RNA-Seq using the company's standard protocols. Raw reads were filtered to remove low quality ones and a total of 1,145,504,498 clean reads were mapped to the *G. hirsutum* TM-1 genome (Zhang *et al.* 2015). The data analysis was performed according to the method described by Cheng *et al.* (2020). Three biological replicates were analyzed for each anther developmental stage.

2.4. Lipid extraction and analysis

Untargeted lipidomics was used to analyze the differences in lipid components of anthers between the WT and MS. Anthers were collected from the WT and MS at four developmental stages and used in lipid extraction according to the methyl tert-butyl ether (MTBE) method (Taguchi and Ishikawa 2010). The lipid extracts were separated using a Nexera LC-30A ultra-high performance liquid chromatography system at Shanghai Applied Protein Technology Co., Ltd. (Shanghai, China), as previously described (Zhu *et al.* 2019). Lipidsearch 4.0 software (Thermo Scientific™, USA) was used for peak detection and annotation of lipids based on internal standards. Finally, the absolute lipid content of the WT and MS anthers was compared based on the results

of mass spectrometry. Each developmental stage was investigated using three biological replicates for both WT and MS.

The lipid molecules significantly different between WT and MS were identified based on the variable weight values obtained by the OPLS-DA Model (variable importance for the projection, VIP), with the criteria of OPLS-DA VIP>1 and *P*-value<0.05.

2.5. Determination of enzyme activity and hydrogen peroxide (H_2O_2) and malondialdehyde (MDA) content

Anthers of MS and WT (0.1 g) were ground into fine powder with a tissue grinder by adding two steel balls into a 2 mL centrifuge tube and immediately cool them with liquid nitrogen. The activities of peroxidase (POD), superoxide dismutase (SOD) and catalase (CAT), as well as the contents of MDA and H_2O_2 were determined according to the protocols described in the kit provided by Suzhou Keming Biotechnology Co., Ltd. (China). All measurement indexes were calculated with three biological replicates by referring to the formulas provided by the kit (Suzhou Keming Biotechnology Co., Ltd.).

2.6. Measurement of fluorescence recovery after photobleaching

The lower epidermis of cotton leaves of MS and WT collected at the pollen maturation stages was peeled off and imaged using a laser confocal microscope (ZEISS LSM 980). The samples were then stained in the FM4-64 fluorescent staining solution for 20 min. Two images were then taken at the time immediately after the 20-min staining and after 60 s recovery. The fluorescence recovery after photobleaching was analyzed based on the images taken before photobleaching, immediately after photobleaching and after 60 s recovery.

2.7. Jasmonic acid (JA) measurement

To investigate the effect of lipid metabolism on the level of JAs, the content of JA and jasmonoyl-isoleucine (JA-ILe) were measured and compared using anthers of MS and WT collected at the pollen maturation stage. JAs were extracted using the method described by Yang (2001) and quantified by using an Enzyme-linked Immunosorbent Assay Kit (Cusabio Life Science, Wuhan, China) following the manufacturer's instructions.

2.8. Observation of Nile red staining

To detect the neutral lipids in anthers of MS and WT, Nile red staining was performed. Cotton anthers were fixed in 2.5% glutaraldehyde for more than 48 h. The sample was processed according to the method described by Gao *et al.* (2014). Photograph was taken using a fluorescent microscope (Nikon Eclipse E100, Japan).

2.9. Fatty acid composition analysis

To analyze the differences in fatty acid components between the WT and MS, anthers of WT and MS were collected from the four developmental stages. The extract supernatant was spiked with an internal standard (25 μL of 500 ppm methyl salicylate), mixed, and subjected to GS-MS using an Agilent Model 7890A/5975C GC-MS System at Applied Protein Technology Co. Ltd. (Shanghai, China). To quantify medium- and long-chain fatty acids, Supelco 37-component FAME (fatty-acid methyl ester) mix (Sigma-Aldrich, the United States) was used to construct a calibration curve for the concentration range of 0.5–1,000 mg L^{-1}. The contents of medium- and long-chain fatty acids were obtained based on GC-MS results using MSD ChemStation software.

2.10. Generating *GhFAD3* mutant by CRISPR/Cas9-mediated gene editing

The *GhFAD3* gene sequence was obtained from the Cotton Functional Genomics Database (https://cottonfgd.org/). Two sgRNAs targeting *GhFAD3* were designed based on the CRISPR-P (http://crispr.hzau.edu.cn/CRISPR2/) and assembled into the pRGEB32-GhU6.7-NPT II expression vector with kanamycin as selection agent. The recombinant vector was transferred to *Agrobacterium tumefaciens* (LBA4404) for cotton transformation with the Upland cotton cv. YZ-1 being the transformation receptor. The pRGEB32-GhU6.7-NPT II expression vector and the Upland cotton cv. YZ-1 were provided by the Cotton Research Institute of Shihezi University. Tissue culture and generation of transgenic plants were carried out following the method described by Liu *et al.* (2019). The primers used in making the CRISPR/Cas9 construct are listed in Appendix A.

2.11. Application of exogenous methyl jasmonate

The methyl jasmonate (MeJA) solution with a concentration of 1,500 μmol L^{-1} MeJA in 0.05% Tween 20 (v/v) was prepared using the method of Fu *et al*. (2015). WT plants were sprayed with the solution every day until the buds opened. As a control, WT plants at the same stages were sprayed with 0.05% Tween 20 (v/v) solution. On the flowering day, anthers and pollen grains were investigated and analyzed.

2.12. Quantitative real-time PCR analysis

Gene specific primers were designed using cDNA sequences of the target genes with the NCBI PrimerBLAST program (Appendix A). qRT-PCR was carried out as described by Cheng *et al.* (2020), using an LightCycler® 480 II (Roche, Switzerland) PCR System. Three independent biological replicates were used for each sample. The relative expression levels were calculated with the cotton ubiquitin gene (GhUBI, XM_012634824) as a reference according to Cheng *et al.* (2020).

2.13. Statistical analysis and building of correlation network

All statistical analyses were conducted by Originpro2018C and GraphPad Prism 8, with the significance levels, * (*P*<0.05) and ** (*P*<0.01), determined by Student's *t*-test.

The differentially expressed genes (DEGs) ($|\log_2 FC| \geq 1$) related to lipid metabolism and the significantly different lipid molecules between WT and MS were used in the Pearson correlation analysis to identify the pairs with a coefficient≥0.9 and *P*-value≤0.05, which were then used in building the correlation network after removing the self-pairing and duplications. The network was constructed and visualized by Cytoscape 3.6.1.

3. Results

3.1. Phenotypic characteristics of the male sterile mutant

No morphological difference in vegetative tissues and organs was observed between WT and MS, but the reproductive tissues and organs of MS were significantly different from those of WT. Compared with WT, MS had smaller petals, larger bracts, shorter stamen filaments, dark yellow anthers, and indehiscent anthers (Fig. 1-A–D). Based on Alexander staining, no pollen grains were produced in MS (Fig. 1-E and F), a result further confirmed by scanning electron microscopy (SEM) observation. Based on SEM, pollen grains in WT anthers were sphere with obvious spinules on the surface, in contrast, no such normal pollen grains but irregularly shaped granules were observed in the MS anthers (Fig. 1-G and H). The phenotypic observations suggest malformation or abortion of pollen grains in MS.

3.2. Transcriptome analysis

To investigate the transcript profile dynamics in MS and WT anthers, we compared transcriptomes of WT and MS anthers of the four developmental stages, i.e., meiosis (MS1/WT1), tetrad (MS2/WT2), mononuclear and binuclear pollen (MS3/WT3), and pollen maturation (MS4/WT4) stages. A total of 22,230 non-redundant DEGs were identified in the four stages, which were enriched with a total of 61 KEGG pathways (Appendices B and C). Among these enrichment pathways were many lipid related pathways, particularly the alpha-linolenic acid metabolism pathway, which was significantly changed in MS at all the four developmental stages of anthers (Fig. 1-I).

3.3. Comparison of lipids during anther development between WT and MS

In order to explore the difference of lipids during anther development between MS and WT, we compared the lipid composition and content in the anthers of MS and WT. A total of 14 different types of lipids were detected in cotton anthers, including seven classes of phospholipids (PC, phosphatidylethanolamine (PE), PA, PI, phosphatidylinositol phosphate (PIP), phosphatidylserine (PS), and PG), two of galactolipids (MGDG and DGDG), two of sphingolipids (Cer and CerG1), two of glycerolipids (DAG and TAG), and free fatty acids (FFAs). Phospholipids were the main lipids in cotton anthers, accounting for more than 60% of the total lipids. Of the phospholipids, PA was the most abundant lipid species. The contents of the other four phospholipids (PI, PIP, PS, and PG) and sphingolipids (Cer and CerG1) in anthers were relatively low. The content of sphingolipids remained stable during the course of anther development, and there was no significant difference between MS and WT. It revealed that PA was the most abundant phospholipid species in anthers and its content was significantly higher in MS than in WT. MGDG and DGDG were the second largest class and their levels were constantly higher in MS. Moreover, MS accumulated significantly more FFAs compared with WT. However, the content of TAG was significantly lower in MS than in WT (Fig. 1-J). Overall, we found abnormal accumulation of PA, MGDG, DGDG, and FFAs, and a significant decrease of TAG in MS, indicating an association between imbalanced lipid metabolism in the MS anthers with the male sterility phenotype.

3.4. Excessive accumulation of PA and FFAs leads to cytotoxicity

It has been reported that excessive accumulation of FFAs and PA is toxic to cells, due to damages to cell membranes, destroying cell signal pathways, and inducing oxidative stress (Li *et al.* 2010; Xu *et al.* 2020). Excessive PA can also produce hydroperoxides and free radicals through a series of enzymes, and eventually lead to membrane lipid peroxidation (Li *et al.* 2009; Ali *et al.* 2022). To investigate whether excessive accumulation of FFAs and PA in MS might cause toxicity, we determined the enzyme activities of POD, SOD and CAT, as well as the contents of H_2O_2 and MDA in WT and MS anthers. The results showed that the activities of POD, SOD and CAT in MS were lower than those in WT (Fig. 2-A). The H_2O_2 and MDA contents, especially the H_2O_2 content, of MS were higher than those of WT (Fig. 2-B). Furthermore, the cell membrane fluidity was determined by fluorescence recovery after photobleaching (FRAP). The fluorescence recovery ratio in the region of interest (ROI) at 60 s was significantly lower in MS (22.10%) than in WT (33.09%) (Fig. 2-C and D). Therefore, the excessive production of FFAs and PA in MS anthers not only caused the imbalance of lipid metabolism, but also led to cytotoxicity and instability of cell membrane.

3.5. Excessive accumulation of MGDG and DGDG increases the level of JA and JA-Ile

JA participates in the final steps of stamen development, such as promoting pollen maturation to ensure pollen viability and fertility, elongating stamen filaments to reach the stigma in preparation for pollination, and controlling anther dehiscence to release pollen grains (Ishiguro *et al.* 2001; von Malek *et al.* 2002). JA is a lipid-derived phytohormone, and its biosynthesis is initiated upon release of C18:3 from MGDG and DGDG of chloroplast membranes (Wasternack and Song 2017). In chloroplast, the released C18:3 is transformed into 12-oxo-phytodienoic acid (OPDA) by a series of enzymatic reactions involving chloroplast-localized lipoxygenase (LOX), allene oxide synthase (AOS), and allene oxide cyclase (AOC) (Bell *et al.* 1995; Stenzel *et al.* 2003; Hyun *et al.* 2008). Then OPDA is translocated into peroxisomes for biosynthesis of JA and JA-Ile (Wasternack and Hause 2013; Yu *et al.* 2020). This study showed that a group of genes of the alpha-linolenic acid metabolism pathway involved in the biosynthesis of JA and its derivatives were significantly up-regulated in MS compared with WT, including genes encoding LOX6 (*Gh_D02G1542*, *Gh_A03G1114*), AOC4 (*Gh_A08G0315*, *Gh_D08G0412*), ACX3 (*Gh_D01G0186*), among others (Fig. 3-A). Consistently, the contents of OPDA, JA and JA-Ile at the pollen maturation stage were significantly higher in MS than in WT (Fig. 3-B). In addition, the MGDG:DGDG ratio was higher in MS than in WT during the development of anthers (Fig. 3-C), in line with the recent finding that an increased MGDG:DGDG ratio is the primary cause of JA overproduction (Yu *et al.* 2020).

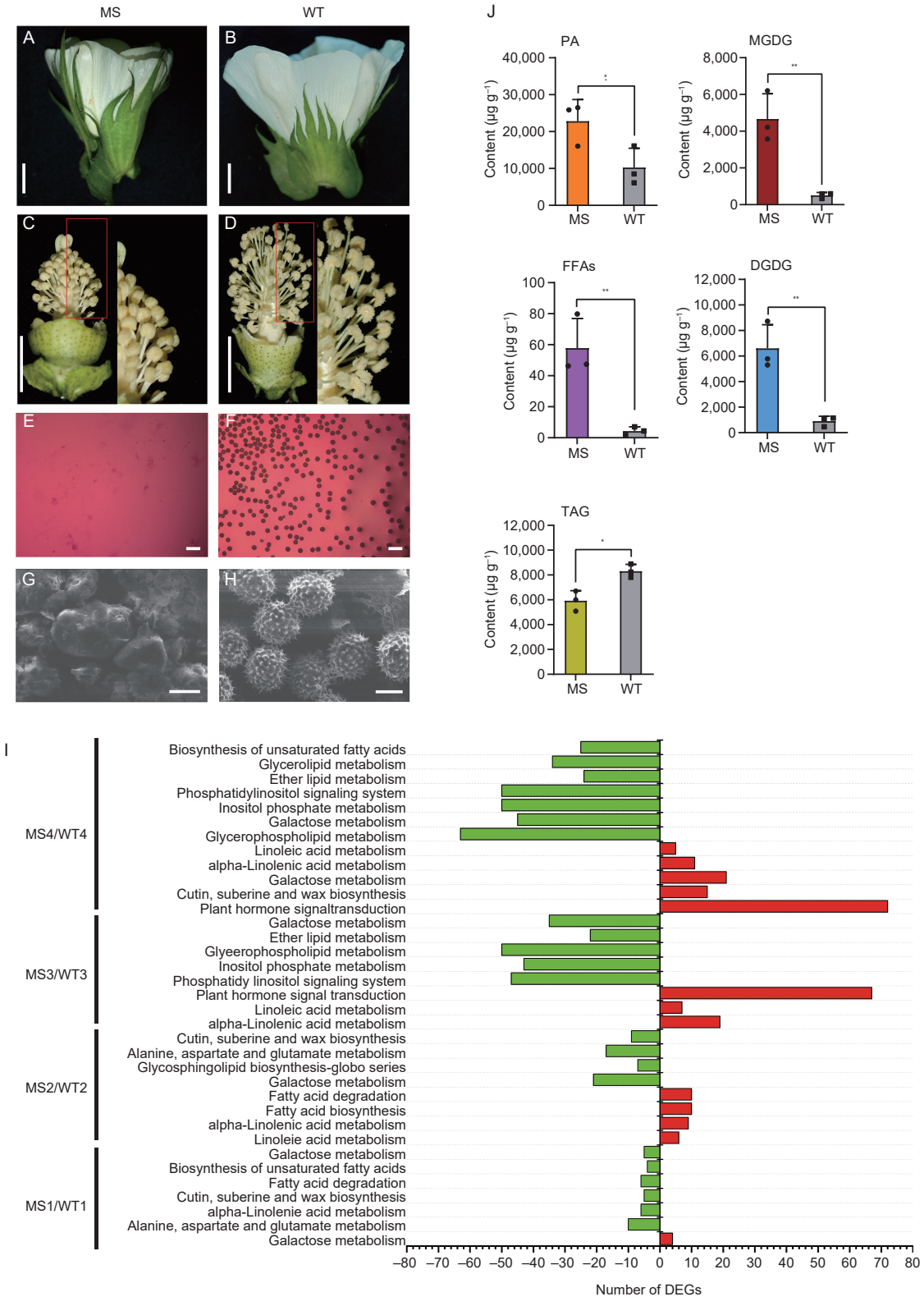


Fig. 1 Comparison of the reproductive organs and the content of the key lipids in anthers between nearly-isogenic male sterile line Shida 98A (MS) and Shida 98 (WT). A and B, 0 days post-anthesis (DPA) flower of MS (A) and WT (B). Scale bars=1 cm. C and D, 0 DPA flower without petals of MS (C) and WT (D). Scale bars=1 cm. E and F, viability of pollen grains from MS (E) and WT (F) based on staining with the Alexander's solution. Scale bars=200 μm. G and H, pollen grains from MS (G) and WT (H) observed by scanning electron microscopy (SEM). Scale bars=20 μm. I, Kyoto encyclopedia of genes and genomes (KEGG) analysis of differentially expressed genes (DEGs) between MS and WT from the four anther development stages. MS1/WT1, meiosis stage; MS2/WT2, tetrad stage; MS3/WT3, mononuclear and binuclear pollen stage; MS4/WT4, pollen maturation stage. J, comparison of the content of phosphatidic acid (PA), free fatty acids (FFAs), triacylglycerol (TAG), monogalactosyldiacylglycerol (MGDG), and digalactosyldiacylglycerol (DGDG) between WT and MS. Values are the mean±SD of three biological replicates. * and ** indicate significant differences at $P<0.05$ and $P<0.01$, respectively, as determined by the Student's *t*-test.

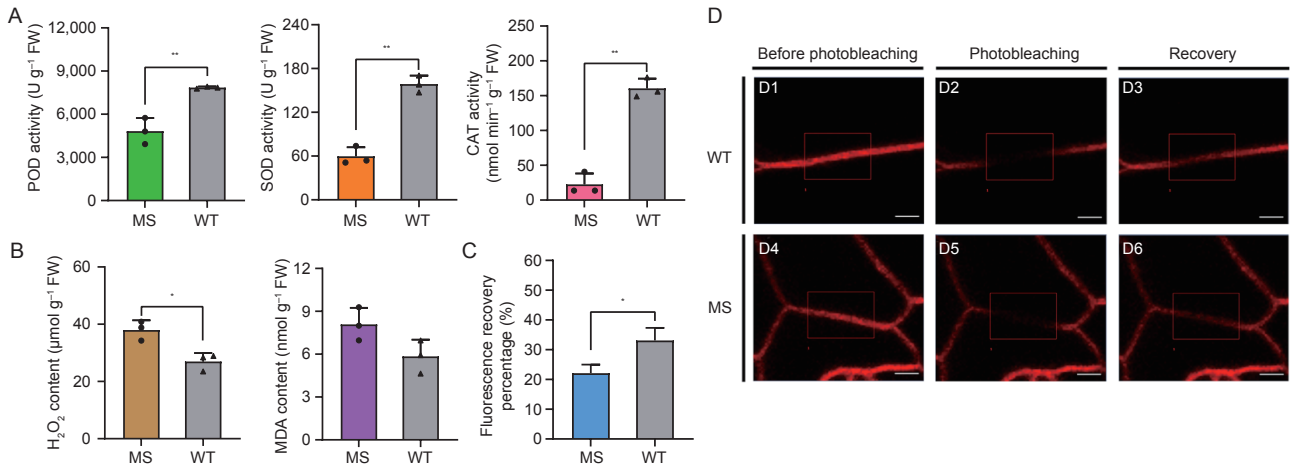


Fig. 2 Activities of peroxidase (POD), superoxide dismutase (SOD) and catalase (CAT), the contents of malondialdehyde (MDA) and hydrogen peroxide (H_2O_2) and the fluidity of cell membrane in the anthers of nearly-isogenic male sterile line Shida 98A (MS) and Shida 98 (WT). A, activities of POD, SOD and CAT in anthers of MS and WT. B, changes of H_2O_2 and MDA contents between MS and WT. Data are means (±SD) from three biological replicates. * and ** indicate significant differences at $P<0.05$ and $P<0.01$, respectively, as determined by the Student's *t*-test. C, fluorescence recovery percentage in MS and WT based on the observation at the regions indicated by the rectangles in D. D, images of FM4-64 staining from MS and WT to compare cell membrane fluidity by fluorescence recovery after photobleaching. D1 and D4 represent the region of interest before photobleaching in WT and MS, respectively, D2 and D5 represent the region of interest after photobleaching in WT and MS, respectively, and D3 and D6 represent the fluorescence recovery of region of interest at 60 s in WT and MS, respectively. Bars=5 μm.

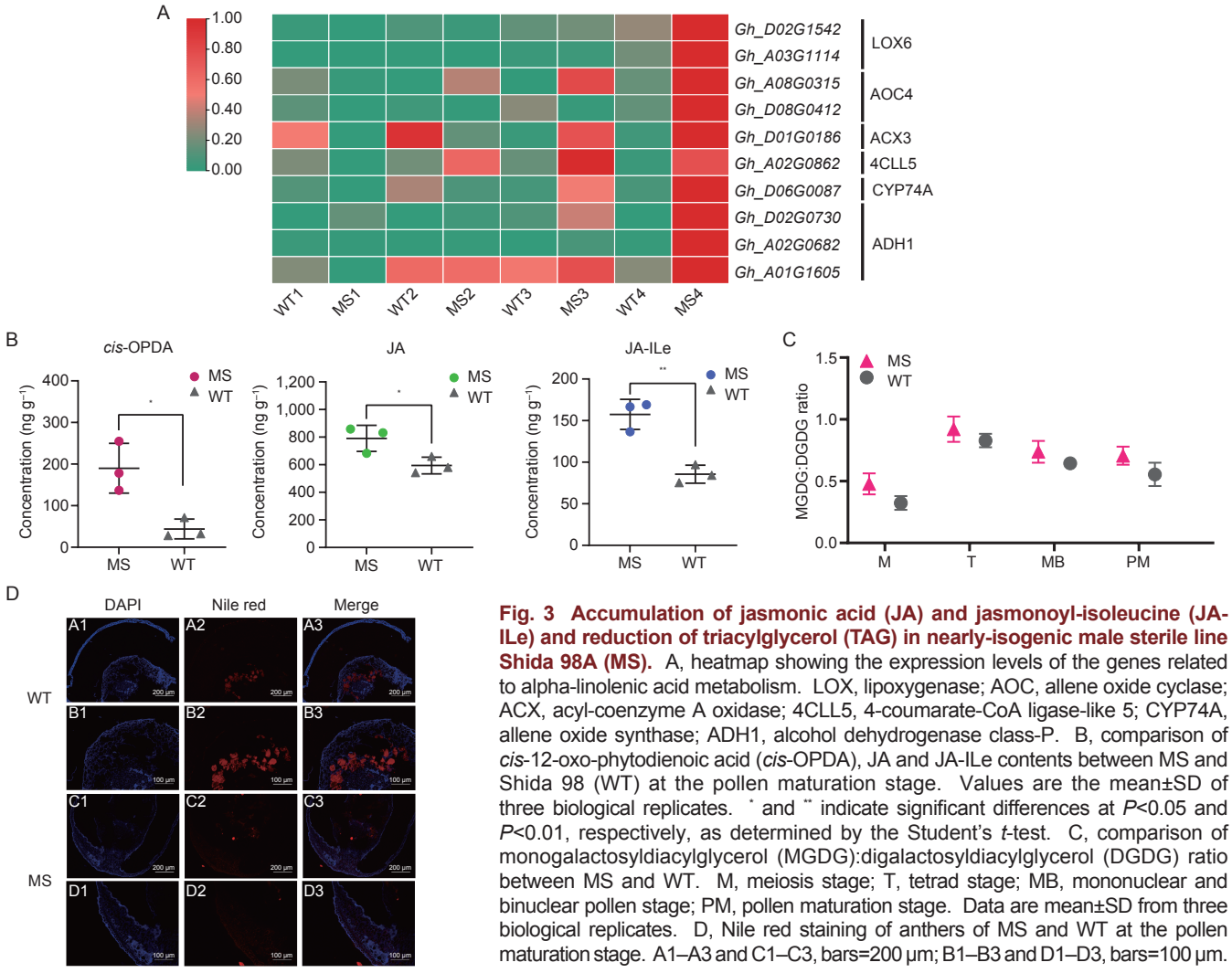


Fig. 3 Accumulation of jasmonic acid (JA) and jasmonoyl-isoleucine (JA-ILe) and reduction of triacylglycerol (TAG) in nearly-isogenic male sterile line Shida 98A (MS). A, heatmap showing the expression levels of the genes related to alpha-linolenic acid metabolism. LOX, lipoxygenase; AOC, allene oxide cyclase; ACX, acyl-coenzyme A oxidase; 4CLL5, 4-coumarate-CoA ligase-like 5; CYP74A, allene oxide synthase; ADH1, alcohol dehydrogenase class-P. B, comparison of *cis*-12-oxo-phytodienoic acid (*cis*-OPDA), JA and JA-ILe contents between MS and Shida 98 (WT) at the pollen maturation stage. Values are the mean±SD of three biological replicates. * and ** indicate significant differences at $P<0.05$ and $P<0.01$, respectively, as determined by the Student's *t*-test. C, comparison of monogalactosyldiacylglycerol (MGDG):digalactosyldiacylglycerol (DGDG) ratio between MS and WT. M, meiosis stage; T, tetrad stage; MB, mononuclear and binuclear pollen stage; PM, pollen maturation stage. Data are mean±SD from three biological replicates. D, Nile red staining of anthers of MS and WT at the pollen maturation stage. A1–A3 and C1–C3, bars=200 μm; B1–B3 and D1–D3, bars=100 μm.

3.6. Excessive reduction in the TAG content is detrimental to anther development

TAG is the main storage form of fatty acids and the main component of vegetable oils (accounting for almost 100%). When anthers were stained with Nile red, an agent for localizing and quantitating lipids, strong red fluorescence signals were clearly visible in the WT mature anthers, but the red fluorescence signals were very weak in the MS mature anthers (Fig. 3-D), indicating that, in the pollen maturation stage, the TAG content was significantly lower in MS than in WT, consistent with the significant decrease of TAG detected by lipidomics (Fig. 1-J). Early study on TAG showed that storage oil bodies with TAG as the main component could provide energy for pollen grain maturation (Piffanelli *et al.* 1998). In addition to serving as a means for efficient carbon and energy storage, TAG plays a critical role in detoxifying FFAs and PA (Yen *et al.* 2008; Kohlwein 2010). The lack of TAG in MS anthers implies that the excessive level of FFAs and PA could not be effectively detoxified, and that not enough energy and nutrition could be provided for pollen grain maturation, leading to failure of anther and pollen development.

3.7. Lipid molecular species containing C18:2 or C18:3-acyl are significantly different between WT and MS

In order to find the lipid component(s) associated with the defects in anther and pollen development, we compared the types of lipid molecules in MS and WT anthers. According to the analysis of lipid molecules, excessive accumulation of PA in MS was mainly contributed by the excess of C34:2-PA (16:0/18:2-PA) and C36:4-PA (18:2/18:2-PA), and their contents were about four times higher in MS than in WT (Fig. 4-A). The content of C36:6-MGDG (C18:3/C18:3-MGDG) and C36:6-DGDG (C18:3/C18:3-DGDG) in MS was about 10 and 7.5 times higher than that in WT, respectively. However, the content of C52:6-TAG (16:0/18:3/18:3-TAG) was significantly lower in MS than in WT (Fig. 4-A). To more intuitively reveal the co-regulatory relationship among the lipid molecules, we built a network showing significantly correlated lipid pairs (Fig. 4-B), which showed that most of the significantly different molecules (OPLS-DA VIP>1 and *P*-value<0.05) between MS and WT contained C18:2 or C18:3-acyl chains. Together, these results indicate that both lipid classes and lipid molecules are significantly different between MS and WT, and that the lipid molecules containing C18:2 or C18:3-acyl chains may be crucial to male fertility.

3.8. Dynamic profiles of fatty acid components in TAG between WT and MS

Fatty acids are mainly stored in TAG. In order to analyze the changes of various fatty acids in TAG in anthers, the absolute content of medium and long chain fatty acids was determined by GC-MS. A total of 38 fatty acid components were identified with palmitic acid (C16:0), oleic acid (C18:1), linoleic acid (C18:2) and alpha-linolenic acid (C18:3) being the main fatty acid components in cotton anthers (Fig. 5). At the M stage, there was no significant difference in oil content (6,012.03 μg g^{-1} for MS and 5,741.84 μg g^{-1} for WT) and fatty acid components between MS and WT. At this stage,

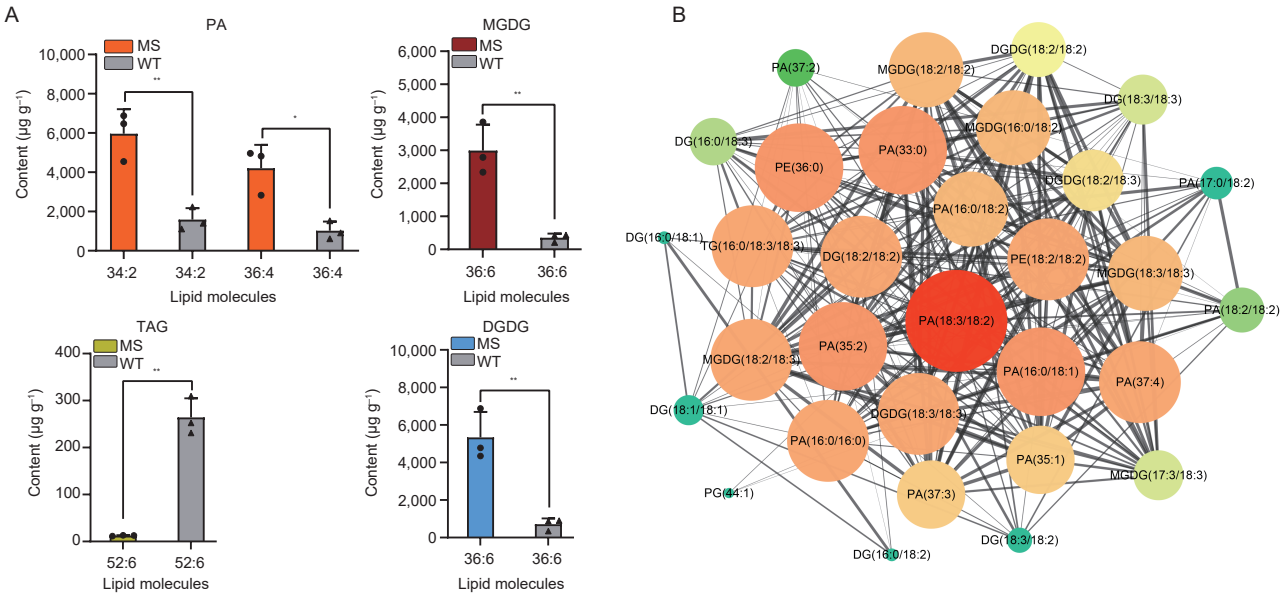


Fig. 4 Comparison of the molecule species of the lipids showing significant difference between nearly-isogenic male sterile line Shida 98A (MS) and Shida 98 (WT). A, comparison of the lipid molecules with significantly different content in MS and WT. Significantly different lipid molecules were selected based on the criteria of OPLS-DA variable importance for the projection (VIP)>1 and *P*<0.05. PA, phosphatidic acid; MGDG, mono-galactosyldiacylglycerol; TAG, triacylglycerol; DGDG, di-galactosyldiacylglycerol. Values are the mean±SD of three biological replicates. * and ** indicate significant differences at *P*<0.05 and *P*<0.01, respectively, as determined by the Student's *t*-test. B, correlation network of the significantly different lipid molecules between MS and WT. Network diagram shows lipid molecule pairs with |*r*|>0.9 and *P*<0.05; correlation degree is indicated by the size (the bigger the stronger) and color (the warmer the stronger) of the circles; thickness of the line represents the absolute value of the correlation coefficient.

the main fatty acid components were C16:0 (19.33% for MS and 19.98% for WT), C18:1 (26.14% for MS and 27.84% for WT), C18:2 (24.07% for MS and 25.65% for WT), and C18:3 (18.75% for MS and 16.45% for WT) (Fig. 5-B). At the T stage, the content of C16:0 was significantly higher in MS than in WT (Fig. 5-A). At the MB stage, C18:1 was one of the main fatty acids in both WT (1,175.26 μg g^{-1}; 21.02%) and MS (1,364.52 μg g^{-1}; 23.16%) and was significantly higher in MS than in WT (Fig. 5-A and B3). In higher plants, C16:0 can extend two carbon atoms to form C18:0 and then to produce C18:1 by dehydrogenation (Liu *et al.* 2017; Rong *et al.* 2022). It seemed that the higher content of C18:1 observed in MS at the MB stage was a result of the increased C16:0 content in MS anthers at the T stage (Fig. 5-A). Finally, at the PM stage, the oil content of MS anthers (5,782.04 μg g^{-1}) was significantly lower than that of WT (8,547.52 μg g^{-1}), mainly due to reduction of C16:0 (867.13 μg g^{-1}, accounting for 15.00% in MS; 1,417.05 μg g^{-1}, accounting for 16.58% in WT) and C18:3 (1,133.61 μg g^{-1}, accounting for 19.61% in MS; 3,105.98 μg g^{-1}, accounting for 36.34% in WT). However, the proportion of C18:1 in the mature anthers of MS (1,362.18 μg g^{-1}, accounting for 23.56%) was much higher than that of

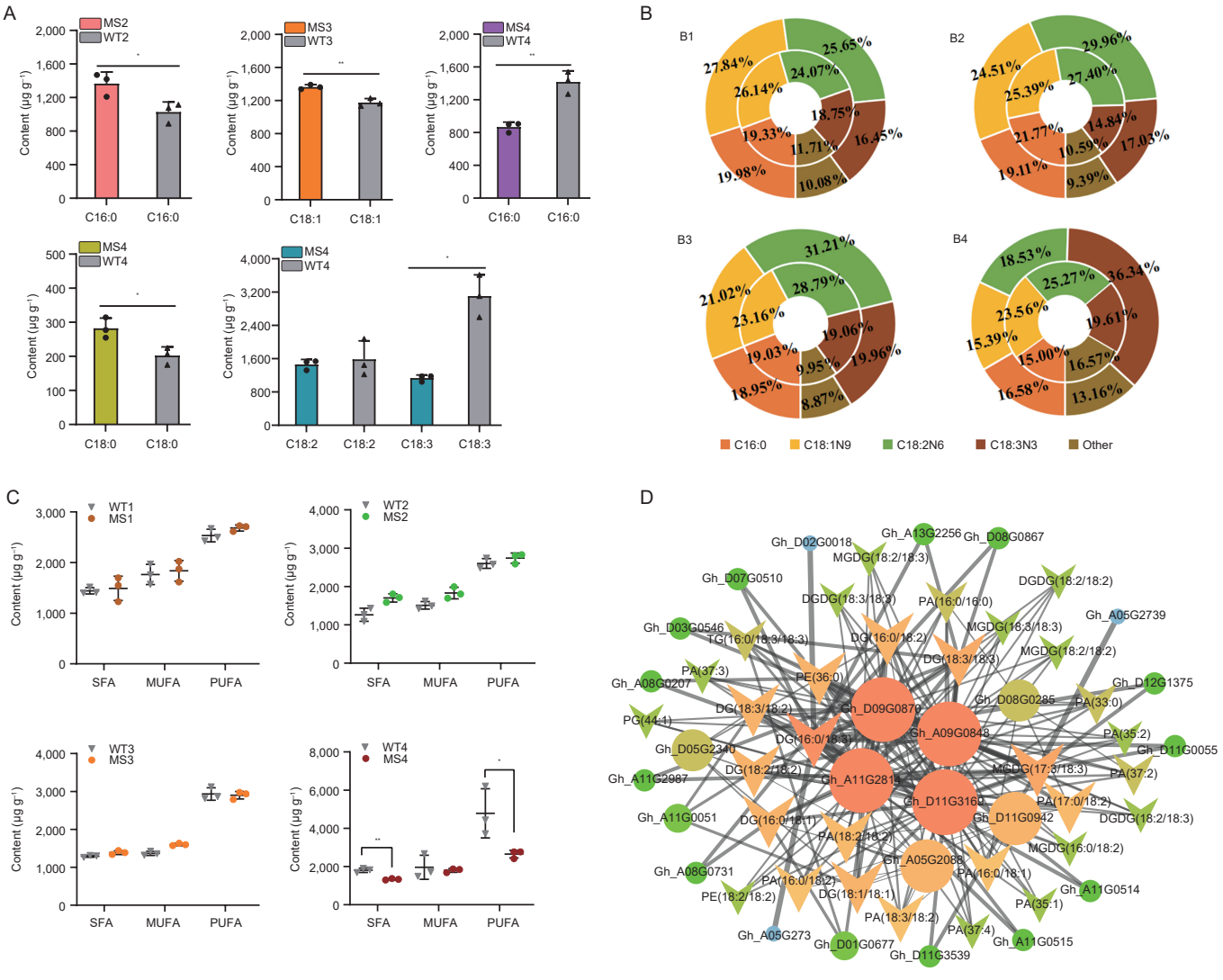


Fig. 5 Comparison of fatty acid components in anthers of nearly-isogenic male sterile line Shida 98A (MS) and Shida 98 (WT) at different developmental stages and correlation between differentially expressed genes (DEGs) and lipid molecules. A, comparison of the contents of different fatty acids between MS and WT. Values are the mean±SD of three biological replicates. * and ** indicate significant differences at $P<0.05$ and $P<0.01$, respectively, as determined by the Student's *t*-test. B, proportion of different fatty acids in anthers of MS and WT at the four anther development stages. The inner ring represents MS and the outer ring represents WT; B1–B4 represent the proportion of fatty acids at meiosis stage, tetrad stage, mononuclear and binuclear pollen stage and pollen maturation stage, respectively. C16:0, palmitic acid; C18:1, oleic acid; C18:2, linoleic acid; C18:3, alpha-linolenic acid. C18:1N9, oleic acid; C18:2N6, linoleic acid; C18:3N3, alpha-linolenic acid. C, comparative analysis of the contents of different saturated fatty acids between MS and WT. SFA, saturated fatty acid; MUFA, monounsaturated fatty acid; PUFA, polyunsaturated fatty acid. D, significant correlation ($|r|>0.9$) between DEGs and significantly different lipid molecules. Circles represent DEGs, triangles represent significantly different lipid molecules. Correlation degree is indicated by the size (the bigger the stronger) and color (the warmer the stronger) of the circles. Thickness of the line represents the absolute value of the correlation coefficient. PA, phosphatidic acid; PE, phosphatidylethanolamine; PG, phosphatidylglycerol; DG, Diacylglycerol. MGDG, mono-galactosyldiacylglycerol; DGDG, di-galactosyldiacylglycerol.

WT (1,315.63 μg g^{-1}, accounting for 15.39%) (Fig. 5-A and B4). In addition, the content of C18:2 in the mature anthers of MS was 1,460.96 μg g^{-1}, lower than 1,584.21 μg g^{-1} in WT (Fig. 5-A). These results suggest that in the biosynthetic steps from C16:0 to C18:1 in MS, more C16:0 was accumulated at the T stage, resulting in more accumulation of C18:1 at the MB stage.

The content of polyunsaturated fatty acids (PUFAs) in MS was only ~half of that in WT at the PM stage (Fig. 5-C). The difference was mainly due to the significant reduction of C18:3 in MS, suggesting that the metabolic pathway from C18:1 to PUFAs was inhibited in MS. High content of C18:1 in cottonseeds had disadvantageous effects on seed vigor (Liu *et al.* 2017), and high accumulation of C18:1 was also unfavorable to the development of anthers (Liu *et al.* 2019). Studies also showed that the decrease of C18:3 content in anther seriously hindered the development of pollen and significantly reduced the number and vitality of pollen grains (McConn and Browse 1996; Weber 2002). Consistently, we found that the content of C18:3, the main component of fatty acids in cotton anthers, was significantly reduced in MS, leading to a very low level of TAG in MS.

3.9. Association between lipid metabolism related DEGs and significantly different lipid molecules

We analyzed the relationship between DEGs related to lipid metabolism and significantly different lipid molecules, and associated DEGs with the lipid molecules that had significantly different level of content (R>0.9) (Fig. 5-D). Based on the network, a group of key genes encoding fatty acid desaturases, namely *FAD2* (*Gh_A11G2814* and *Gh_D11G3169*) and *FAD3* (*Gh_A09G0848* and *Gh_D09G0870*), were significantly associated with more than 30 lipid molecules. These genes were significantly down-regulated in MS, hindering the continuous desaturation of fatty acids and consequently reducing the content of C18:3 in MS (Appendix D; Fig. 5-A). Notably, most of the significantly different lipid molecules in the network contain C18:3-acyl chains, implying the importance of the lipid molecules (PA, MGDG, DGDG, and TAG) containing C18:3-acyl chains in cotton anther development.

3.10. Knock-out *GhFAD3* leads to male sterility

Through the comprehensive analysis of lipid metabolism, C18:3 derived from catalyzation of C18:2 by FAD3 seemed to play an important role in cotton anther development. We thus investigated the effect of loss-of-function of *GhFAD3* on anther development. *GhFAD3* mutants were generated using CRISPR-Cas9-mediated gene editing using two sgRNAs (501 bp away from each other) targeting the 1st and 4th exons of both *GhFAD3* genes (Fig. 6-A and B). Four edited lines (*ghfad3* mutants) were identified from a total of 21 transgenic plants based on sequencing of the target sites (Fig. 6-C). Compared with WT (YZ-1), all *ghfad3* mutants exhibited defects in the reproductive organs, exhibiting

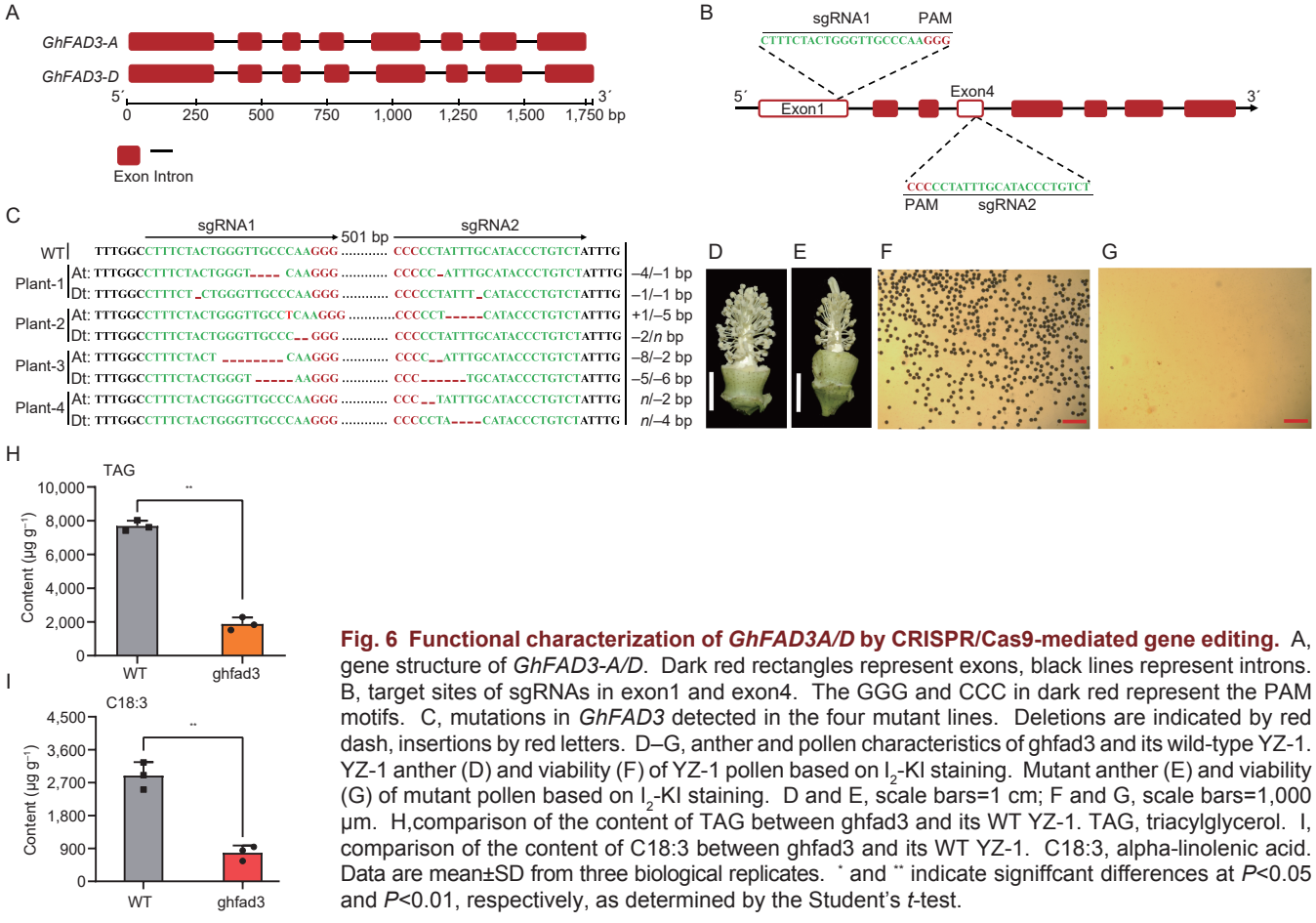


Fig. 6 Functional characterization of *GhFAD3A/D* by CRISPR/Cas9-mediated gene editing. A, gene structure of *GhFAD3-A/D*. Dark red rectangles represent exons, black lines represent introns. B, target sites of sgRNAs in exon1 and exon4. The GGG and CCC in dark red represent the PAM motifs. C, mutations in *GhFAD3* detected in the four mutant lines. Deletions are indicated by red dash, insertions by red letters. D–G, anther and pollen characteristics of ghfad3 and its wild-type YZ-1. YZ-1 anther (D) and viability (F) of YZ-1 pollen based on I_2-KI staining. Mutant anther (E) and viability (G) of mutant pollen based on I_2-KI staining. D and E, scale bars=1 cm; F and G, scale bars=1,000 μm. H,comparison of the content of TAG between ghfad3 and its WT YZ-1. TAG, triacylglycerol. I, comparison of the content of C18:3 between ghfad3 and its WT YZ-1. C18:3, alpha-linolenic acid. Data are mean±SD from three biological replicates. * and ** indicate signiffcant differences at P<0.05 and P<0.01, respectively, as determined by the Student's t-test.

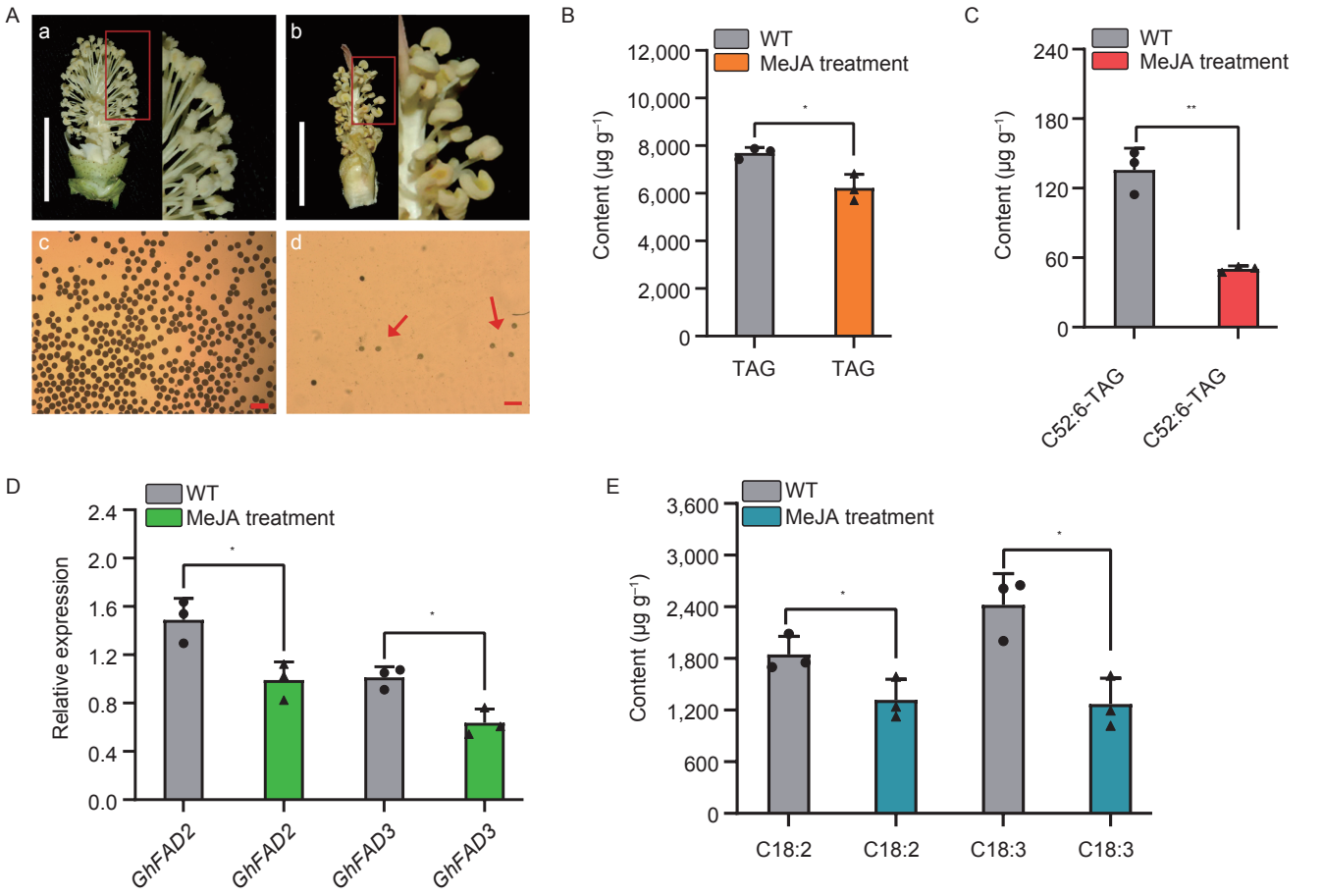


Fig. 7 Exogenous jasmonic acid (JA) treatment damaged pollen fertility. A, anthers of methyl jasmonate (MeJA)-treated (b) and control plants (a). Scale bars=1 cm. Pollen grains of control plants (c) and MeJA-treated (d) stained with I_2-KI. Scale bars=200 μm. B, triacylglycerol (TAG) content in the anthers of MeJA-treated plants and control plants. C, content of TAG molecules in the anthers of MeJA-treated plants and control plants. D, qRT-PCR analysis of the expression level of *GhFAD2* and *GhFAD3* in the anthers of MeJA-treated plants and control plants. E, contents of C18:2 (linoleic acid) and C18:3 (alpha-linolenic acid) in the anthers of MeJA-treated plants and control plants. Values are the mean±SD of three biological replicates. * and ** indicate significant differences at $P<0.05$ and $P<0.01$, respectively, as determined by the Student's *t*-test.

shorter stamen filaments, smaller anthers, and longer stigma (Fig. 6-D and E), as well as lack of viable pollen grains based on I_2-KI staining (Fig. 6-F and G). TAG and C18:3 contents were significantly reduced in the anthers of *ghfad3* mutants (Fig. 6-H and I). The result indicated that *GhFAD3* is essential for development of cotton anthers and pollen grains.

3.11. Exogenous JA treatment damages pollen fertility

The content of JA and JA-ILe was significantly higher in MS anthers than in WT anthers (Fig. 3-B). To know the effect of excessive JA on male fertility, exogenous MeJA was applied to flower buds of WT plants. After the application of MeJA solution, cotton anthers produced few pollen grains based on I_2-KI staining and no pollen was released from the anthers (Fig. 7-A). Due to feedback regulation of JA, the contents of MGDG and DGDG were significantly decreased (Appendix E). It was noteworthy that TAG and C52:6-TAG (16:0/18:3/18:3-TAG) contents were significantly reduced in anthers from the MeJA-treated plants compared to the untreated plants (Fig. 7-B and C). *GhFAD2* and *GhFAD3* expression levels, as well as C18:2 and C18:3 contents were also significantly reduced in the anthers from the MeJA-treated plants compared with the untreated plants (Fig. 7-D and E). These results imply that excessive JA may inhibit *GhFAD2* and *GhFAD3* expression in a feedback manner, resulting in a significant decrease of C18:2 and C18:3, which further inhibited C52:6-TAG synthesis.

4. Discussion

4.1. Excessive accumulation of FFAs, PA, MGDG and DGDG and the lack of TAG cause lipid metabolism imbalance and affect cotton male fertility

Lipid is an indispensable component of anther structure, so proper lipid metabolism is very important for anther development. On the one hand, we found that MS anthers had an excessive accumulation of FFAs and PA. Increasing numbers of studies have proved that excessive PA can produce hydroperoxides and free radicals by a series of enzymes, and eventually lead to membrane lipid peroxidation (Li *et al.* 2009; Ali *et al.* 2022). Moreover, the excessive accumulation of FFAs and PA is toxic to cells, and can destabilize cellular membranes, disrupt cellular signaling pathways, and induce oxidative stress and even cell death (Li *et al.* 2010; Xu *et al.* 2020). Consistent with the result of

excessive accumulation of FFAs and PA in MS, the content of H_2O_2 and MDA was significantly higher in MS than in WT (Figs. 1-J and 2-B). This finding is consistent to those observed in other male sterility studies (Mittler 2002; Jiang *et al.* 2007; Xie *et al.* 2014). The enzyme activities of POD, SOD and CAT were lower in MS than in WT (Fig. 2-A). Taken together, the excessive accumulation of FFAs and PA produced more H_2O_2 and MDA, which is detrimental to the development of anthers by destroying the stability of cell membrane.

On the other hand, TAG biosynthesis pathway was inhibited in MS, resulting in insufficient TAG content (Fig. 1-J). Early studies on TAG showed that storage oil bodies with TAG as the main component provides energy for pollen grain maturation (Piffanelli *et al.* 1998). Studies in yeast and mammalians also clearly showed that, in addition to serving as a means for efficient carbon and energy storage, TAG plays a critical role in detoxifying FFAs and PA (Yen *et al.* 2008; Kohlwein 2010). In *Brassica napus* and *Arabidopsis thaliana*, it was also indirectly proved that TAG protects cells against lipotoxic damage (Lock *et al.* 2009; Zhang *et al.* 2009; Fan *et al.* 2013). The cotton male sterile line (MS) investigated in this study could not effectively detoxify excessive FFAs and PA and provide energy and nutrients for pollen grain maturation due to the lack of TAG, causing a negative impact on anther development. In addition, fatty acids are mainly stored in TAG. PUFAs sequestered in TAG of the oil bodies are less susceptible to ROS induced lipid peroxidation, thereby buffering lipid homeostasis (Bailey *et al.* 2015; Xu *et al.* 2020).

4.2. *GhFAD3* plays a critical role in cotton anther development

In the previous studies of cotton male sterility, it was found that an abnormal fatty acid pathway is associated with the formation of defective pollen walls in anthers, and it was further found that the fatty acid synthesis pathway was inhibited and the oxidation pathway of long-chain fatty acids was activated (Wu *et al.* 2015, 2019). We analyzed the content of 38 fatty acids and found that C18:3 content in MS was reduced by nearly three times compared to that in WT (Fig. 5-A). Our findings showed that genes encoding FAD2 and FAD3 were significantly down-regulated in MS, consistent with the significant reduction of the C18:3 content in MS. In cottonseed oil, the content of C18:3 is very low, accounting for only about 0.3%. Unlike cottonseed and other cotton tissues, cotton anthers have a high content of C18:3, indicating that *GhFAD3* may play a very important role in cotton anther development. C18:3 is crucial for pollen development and anther dehiscence in *A. thaliana* and C18:3 achieves its function *via* serving as the substrate for JA biosynthesis through the octadecanoid pathway (McConn and Browse 1996). In *Arabidopsis*, the loss-of-function mutants of the JA synthesis-related genes, such as *AtOPR3*, *AtAOS*, *AtLOX3*/*AtLOX4*, and *AtACX1*/*AtACX5*, showed variable level of defects in anther dehiscence, filament elongation and pollen maturation, leading to male sterility (Stintzi and Browse 2000; Park *et al.* 2002; Schilmiller *et al.* 2007; Caldelari *et al.* 2011; Wan *et al.* 2020). We found that the *ghfad3* mutants generated by gene editing exhibited developmental defects in anthers and pollen grains (Fig. 6-E and G).

In cotton, the auxin level in anthers must be maintained at a certain level to ensure normal anther development, because too high or too low auxin level leads to male sterility under the high temperature conditions (Min *et al.* 2014; Ding *et al.* 2017). Like auxin, it seems that the JA level needs to be well-balanced in anther as well to ensure proper development of anthers. Unlike previous reports of insufficient JA leading to male sterility (Ishiguro *et al.* 2001; Park *et al.* 2002; Khan *et al.* 2020), our study found that exogenous spraying JA led to defects in pollen development and anther indehiscence (Fig. 7-A). Similarly, the male fertility of the *ghfad2-3* mutants could not be restored by the application of exogenous JA, and unusual FA products including epoxidation, hydroxylation and double bonding conjugation inhibit the activity of FAD2, thereby effectively preventing the conversion of C18:1 to C18:2 (Liu *et al.* 2019). These results imply that balanced lipid metabolism and the homeostasis of phytohormones, such as auxin and JA, in anthers are critical for anther development and male fertility.

Interestingly, lipid molecules containing C18:3-acyl chains bound to MGDG and DGDG were significantly higher in MS than in WT (Fig. 4-A). In some crops, unlike C16:3 plants such as *Arabidopsis*, the synthesis of plastid lipids almost completely depends on the eukaryotic pathway, and the product of this process contains a large amount of 18:3 fatty acids, resulting in dominating C36:6 (C18:3/C18:3) molecule species in their MGDG and DGDG, thus they are called 18:3 plants (Heinz and Roughan 1983; Browse *et al.* 1986; Lohden and Frentzen 1988; Ohlrogge and Browse 1995). In our study, C36:6 is indeed dominant in MGDG and DGDG, which is consistent with the characteristics of typical 18:3 plants. TAG is synthesized in the ER. In ER, C18:2 is produced by catalysis of fatty acid desaturases FAD2, and is further desaturated to form C18:3 by FAD3. MGDG and DGDG are synthesized in plastids. In the plastids of MS, the desaturation process catalyzed by GhFAD7 (Yurchenko *et al.* 2014), which was not restricted. In both ER and plastids, PA is the precursor of other phospholipids. As a synthetic substrate of MGDG, PA activates the extensive synthesis of MGDG and DGDG in early anther development. TAG is mainly synthesized in the late stage through PA by the Kennedy pathway. Due to the desaturation pathway deficiency in ER, the lower levels of TAG and higher levels of MGDG and DGDG were observed in MS. The abnormal accumulation of JA synthesized by C36:6-MGDG and C36:6-DGDG as substrates in MS, and excessive JA may feedback inhibit *GhFAD3* expression led to a significant decrease in C18:3 content in MS, further hindering TAG synthesis and exacerbating TAG deficiency in the later stage. This imbalanced lipid metabolism in anther, mainly due to the disorder of the alpha-linolenic acid metabolism affected anthers development and ultimately led to male sterility (Fig. 8). Taken together, C18:3 is the important substrate for biosynthesis of many other lipids and plays important roles in lipid metabolism balance of cotton anther. Analyses of C18:3 function may expand a deep understanding of the physiological significance of the balanced lipid metabolism in cells and would help us to better control plant growth and development.

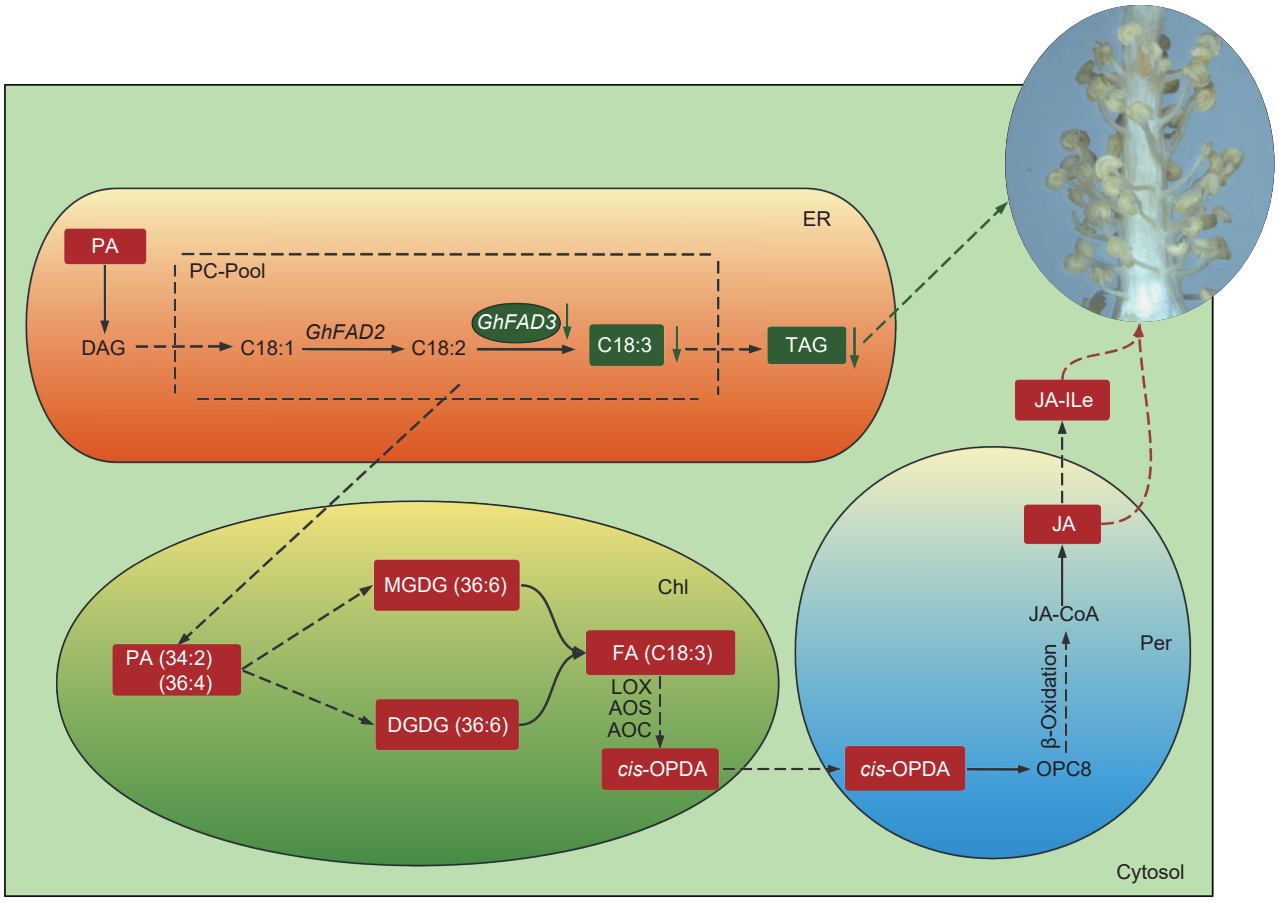


Fig. 8 A proposed scheme showing the comprehensive role of alpha-linolenic acid metabolism in regulating cotton male fertility. The metabolites with a higher content and a lower content in nearly-isogenic male sterile line Shida 98A (MS) than in wild-type Shida 98 (WT) are highlighted with red and green boxes, respectively. ER, endoplasmic reticulum; Chl, chloroplast; Per, peroxisome; PA, phosphatidic acid; DAG, diacylglycerol; C18:1, oleic acid; C18:2, linoleic acid; C18:3, alpha-linolenic acid; TAG, triacylglycerol; MGDG, monogalactosyldiacylglycerol; DGDG, digalactosyldiacylglycerol; FA, fatty acid; *cis*-OPDA, *cis*-12-oxo-phytodienoic acid; JA, jasmonic acid JA-ILe, jasmonoyl-isoleucine.

5. Conclusion

In this study, we conducted a comprehensive analysis of lipid metabolism in cotton anthers. We demonstrated that the accumulation of C18:3 plays a crucial role in balanced lipid metabolism and male fertility. The results showed that the MS anthers over-accumulated FFAs, PA, MGDG, and DGDG, while had a decreased content of TAG, which was closely related to the abnormal metabolism of C18:3. Furthermore, it was found that JA also accumulated excessively, and its substrate comes from C18:3 released by MGDG and DGDG. The verification of the C18:3 synthesis gene indicated the important role of C18:3 in anther development. Our study revealed the importance of lipid metabolism balance in regulating male fertility.

Acknowledgements

This work was supported by the Science and Technology Major Program of Bingtuan, China (2023AA008), the National Natural Science Foundation of China (31960369), the Bingtuan Science and Technology Program, China (2025DA001), and the Henan Provincial Science and Technology Research Project, China (222102110200).

Declaration of competing interest

The authors declare that they have no conflict of interest.

Declaration of generative AI and AI-assisted technologies in the writing process

The authors declare that they did not use AI in the preparation and writing of this manuscript.

Appendices associated with this paper are available at https://doi.org/10.1016/j.jia.2024.07.036

References

Ali U, Lu S, Fadlalla T, Iqbal S, Yue H, Yang B, Hong Y, Wang X, Guo L. 2022. The functions of phospholipases and their hydrolysis products in plant growth, development and stress responses. *Progress in Lipid Research*, **86**, 101158.

Bailey A P, Koster G, Guillermier C, Hirst E M, MacRae J I, Lechene C P, Postle A D, Gould A P. 2015. Antioxidant role for lipid droplets in a stem cell niche of drosophila. *Cell*, **163**, 340–353.

Bates P D. 2016. Understanding the control of acyl flux through the lipid metabolic network of plant oil biosynthesis. *Biochimica et Biophysica Acta*, **1861**, 1214–1225.

Bell E, Creelman R A, Mullet J E. 1995. A chloroplast lipoxygenase is required for wound-induced jasmonic acid accumulation in

Arabidopsis. *Proceedings of the National Academy of Sciences of the United States of America*, **92**, 8675–8679.
Benning C. 2009. Mechanisms of lipid transport involved in organelle biogenesis in plant cells. *Annual Review of Cell and Developmental Biology*, **25**, 71–91.
Block M A, Dorne A J, Joyard J, Douce R. 1983. Preparation and characterization of membrane fractions enriched in outer and inner envelope membranes from spinach chloroplasts. I. Electrophoretic and immunochemical analyses. *Journal of Biological Chemistry*, **258**, 13273–13280.
Browse J, Warwick N, Somerville C R, Slack C R. 1986. Fluxes through the prokaryotic and eukaryotic pathways of lipid synthesis in the '16:3' plant *Arabidopsis thaliana*. *The Biochemical Journal*, **235**, 25–31.
Caldelari D, Wang G, Farmer E E, Dong X. 2011. *Arabidopsis* lox3 lox4 double mutants are male sterile and defective in global proliferative arrest. *Plant Molecular Biology*, **75**, 25–33.
Cheng X Q, Zhang X Y, Xue F, Zhu S H, Li Y J, Zhu Q H, Liu F, Sun J. 2020. Characterization and transcriptome analysis of a dominant genic male sterile cotton mutant. *BMC Plant Biology*, **20**, 312.
Ding Y, Ma Y, Liu N, Xu J, Hu Q, Li Y, Wu Y, Xie S, Zhu L, Min L, Zhang X. 2017. microRNAs involved in auxin signalling modulate male sterility under high-temperature stress in cotton (*Gossypium hirsutum*). *The Plant Journal*, **91**, 977–994.
Fan J, Yan C, Xu C. 2013. Phospholipid: Diacylglycerol acyltransferase-mediated triacylglycerol biosynthesis is crucial for protection against fatty acid-induced cell death in growing tissues of *Arabidopsis*. *The Plant Journal*, **76**, 930–942.
Fu W, Shen Y, Hao J, Wu J, Ke L, Wu C, Huang K, Luo B, Xu M, Cheng X, Zhou X, Sun J, Xing C, Sun Y. 2015. Acyl-CoA N-acyltransferase influences fertility by regulating lipid metabolism and jasmonic acid biogenesis in cotton. *Scientific Reports*, **5**, 11790.
Gao Y, Chen G, Weselake R J. 2014. A rapid nile red fluorescence-based method for triacylglycerol content in microspore-derived cell suspension cultures of *Brassica napus*. *Lipids*, **49**, 1161–1168.
Han G S, Carman G M. 2010. Characterization of the human LPIN1-encoded phosphatidate phosphatase isoforms. *The Journal of Biological Chemistry*, **285**, 14628–14638.
He M, Ding N Z. 2020. Plant unsaturated fatty acids: Multiple roles in stress response. *Frontiers in Plant Science*, **11**, 562785.
Heinz E, Roughan P G. 1983. Similarities and differences in lipid metabolism of chloroplasts isolated from 18:3 and 16:3 plants. *Plant Physiology*, **72**, 273–279.
Hyun Y, Choi S, Hwang H J, Yu J, Nam S J, Ko J, Park J Y, Seo Y S, Kim E Y, Ryu S B, Kim W T, Lee Y H, Kang H, Lee I. 2008. Cooperation and functional diversification of two closely related galactolipase genes for jasmonate biosynthesis. *Developmental Cell*, **14**, 183–192.
Ishiguro S, Kawai-Oda A, Ueda J, Nishida I, Okada K. 2001. The *DEFECTIVE IN ANTHER DEHISCIENCE1* gene encodes a novel phospholipase A1 catalyzing the initial step of jasmonic acid biosynthesis, which synchronizes pollen maturation, anther dehiscence, and flower opening in *Arabidopsis*. *The Plant Cell*, **13**, 2191–2209.
Jiang P, Zhang X, Zhu Y, Zhu W, Xie H, Wang X. 2007. Metabolism of reactive oxygen species in cotton cytoplasmic male sterility and its restoration. *Plant Cell Reports*, **26**, 1627–1634.
Khan A H, Min L, Ma Y, Wu Y, Ding Y, Li Y, Xie S, Ullah A, Shaban M, Manghwar H, Shahid M, Zhao Y, Wang C, Zhang X. 2020. High day and night temperatures distinctively disrupt fatty acid and jasmonic acid metabolism, inducing male sterility in cotton. *Journal of Experimental Botany*, **71**, 6128–6141.
Kohlwein S D. 2010. Triacylglycerol homeostasis: Insights from yeast. *The Journal of Biological Chemistry*, **285**, 15663–15667.
Lavell A A, Benning C. 2019. Cellular organization and regulation of plant glycerolipid metabolism. *Plant Cell Physiology*, **60**, 1176–1183.
Li L O, Klett E L, Coleman R A. 2010. Acyl-CoA synthesis, lipid metabolism and lipotoxicity. *Biochimica et Biophysica Acta*, **1801**, 246–251.
Li M, Hong Y, Wang X. 2009. Phospholipase D- and phosphatidic acid-mediated signaling in plants. *Biochimica et Biophysica Acta*, **1791**, 927–935.
Li-Beisson Y, Shorrosh B, Beisson F, Andersson M X, Arondel V, Bates P D, Baud S, Bird D, Debono A, Durrett T P, Franke R B, Graham I A, Katayama K, Kelly A A, Larson T, Markham J E, Miquel M, Molina I, Nishida I, Rowland O, *et al.* 2013. Acyl-lipid metabolism. *The Arabidopsis Book*, **11**, e0161.
Liu F, Ma L, Wang Y, Li Y, Zhang X, Xue F, Nie X, Zhu Q, Sun J. 2019. *GhFAD2-3* is required for anther development in *Gossypium hirsutum*. *BMC Plant Biology*, **19**, 393.
Liu F, Zhao Y P, Zhu H G, Zhu Q H, Sun J. 2017. Simultaneous silencing of *GhFAD2-1* and *GhFATB* enhances the quality of cottonseed oil with high oleic acid. *Journal of Plant Physiology*, **215**, 132–139.
Lock Y Y, Snyder C L, Zhu W, Siloto R M, Weselake R J, Shah S. 2009. Antisense suppression of type 1 diacylglycerol acyltransferase adversely affects plant development in *Brassica napus*. *Physiologia Plantarum*, **137**, 61–71.
Lohden I, Frentzen M. 1988. Role of plastidial acyl-acyl carrier protein: Glycerol 3-phosphate acyltransferase and acyl-acyl carrier protein hydrolase in channelling the acyl flux through the prokaryotic and eukaryotic pathway. *Planta*, **176**, 506–512.
Ma H, Wu Y, Lv R, Chi H, Zhao Y, Li Y, Liu H, Ma Y, Zhu L, Guo X, Kong J, Wu J, Xing C, Zhang X, Min L. 2022. Cytochrome P450 mono-oxygenase CYP703A2 plays a central role in sporopollenin formation and ms5ms6 fertility in cotton. *Journal of Integrative Plant Biology*, **64**, 2009–2025.
von Malek B, van der Graaff E, Schneitz K, Keller B. 2002. The *Arabidopsis* male-sterile mutant *dde2-2* is defective in the *ALLENE OXIDE SYNTHASE* gene encoding one of the key enzymes of the jasmonic acid biosynthesis pathway. *Planta*, **216**, 187–192.
Maraschin F, Kulcheski F R, Segatto A, Trenz T S, Barrientos-Diaz O, Margis-Pinheiro M, Margis R, Turchetto-Zolet A C. 2019. Enzymes of glycerol-3-phosphate pathway in triacylglycerol synthesis in plants: Function, biotechnological application and evolution. *Progress in Lipid Research*, **73**, 46–64.
McConn M, Browse J. 1996. The critical requirement for linolenic acid is pollen development, not photosynthesis, in an *Arabidopsis* mutant. *The Plant Cell*, **8**, 403–416.
Min L, Li Y, Hu Q, Zhu L, Gao W, Wu Y, Ding Y, Liu S, Yang X, Zhang X. 2014. Sugar and auxin signaling pathways respond to high-temperature stress during anther development as revealed by transcript profiling analysis in cotton. *Plant Physiology*, **164**, 1293–1308.
Mittler R. 2002. Oxidative stress, antioxidants and stress tolerance. *Trends in Plant Science*, **7**, 405–410.
Ohlrogge J, Browse J. 1995. Lipid biosynthesis. *The Plant Cell*, **7**, 957–970.
Park J H, Halitschke R, Kim H B, Baldwin I T, Feldmann K A, Feyereisen R. 2002. A knock-out mutation in allene oxide synthase results in male sterility and defective wound signal transduction in *Arabidopsis* due to a block in jasmonic acid biosynthesis. *The Plant Journal*, **31**, 1–12.
Piffanelli P, Ross J H, Murphy D. 1998. Biogenesis and function of the lipidic structures of pollen grains. *Sexual Plant Reproduction*, **11**, 65–80.
Pressman E, Shaked R, Shen S, Altahan L, Firon N. 2012. Variations in carbohydrate content and sucrose-metabolizing enzymes in tomato (*Solanum lycopersicum* L.) stamen parts during pollen maturation. *American Journal of Plant Sciences*, **3**, 252–260.
Rong H, Yang W, Xie T, Wang Y, Wang X, Jiang J, Wang Y. 2022. Transcriptional profiling between yellow- and black-seeded *Brassica napus* reveals molecular modulations on flavonoid and fatty acid content. *Journal of Integrative Agriculture*, **21**, 2211–2226.
Sawhney V K, Shukla S A. 1994. Male sterility in flowering plants: Are plant growth substances involved. *American Journal of Botany*, **81**, 1640–1647.
Schilmiller A L, Koo A J, Howe G A. 2007. Functional diversification of acyl-coenzyme A oxidases in jasmonic acid biosynthesis and action. *Plant Physiology*, **143**, 812–824.
Stenzel I, Hause B, Miersch O, Kurz T, Maucher H, Weichert H, Ziegler J, Feussner I, Wasternack C. 2003. Jasmonate biosynthesis and the allene oxide cyclase family of *Arabidopsis thaliana*. *Plant Molecular Biology*, **51**, 895–911.
Stintzi A, Browse J. 2000. The *Arabidopsis* male-sterile mutant, opr3, lacks the 12-oxophytodienoic acid reductase required for jasmonate synthesis. *Proceedings of the National Academy of Sciences of the United States of America*, **97**, 10625–10630.
Taguchi R, Ishikawa M. 2010. Precise and global identification

of phospholipid molecular species by an Orbitrap mass spectrometer and automated search engine lipid search. *Journal of Chromatography A*, **1217**, 4229–4239.
Vance J E, Vance D E. 2004. Phospholipid biosynthesis in mammalian cells. *Biochemistry and Cell Biology*, **82**, 113–128.
Wan X, Wu S, Li Z, An X, Tian Y. 2020. Lipid metabolism: Critical roles in male fertility and other aspects of reproductive development in plants. *Molecular Plant*, **13**, 955–983.
Wasternack C, Hause B. 2013. Jasmonates: Biosynthesis, perception, signal transduction and action in plant stress response, growth and development. *Annals of Botany*, **111**, 1021–1058.
Wasternack C, Song S. 2017. Jasmonates: Biosynthesis, metabolism, and signaling by proteins activating and repressing transcription. *Journal of Experimental Botany*, **68**, 1303–1321.
Weber H. 2002. Fatty acid-derived signals in plants. *Trends in Plant Science*, **7**, 217–224.
Wu Y, Li Y, Li Y, Ma Y, Zhao Y, Wang C, Chi H, Chen M, Ding Y, Guo X, Min L, Zhang X. 2019. Proteomic analysis reveals that sugar and fatty acid metabolisms play a central role in sterility of the male-sterile line 1355A of cotton. *The Journal of Biological Chemistry*, **294**, 7057–7067.
Wu Y, Min L, Wu Z, Yang L, Zhu L, Yang X, Yuan D, Guo X, Zhang X. 2015. Defective pollen wall contributes to male sterility in the male sterile line 1355A of cotton. *Scientific Reports*, **5**, 9608.
Xie H T, Wan Z Y, Li S, Zhang Y. 2014. Spatiotemporal production of reactive oxygen species by NADPH oxidase is critical for tapetal programmed cell death and pollen development in *Arabidopsis*. *The Plant Cell*, **26**, 2007–2023.
Xu C, Fan J, Shanklin J. 2020. Metabolic and functional connections between cytoplasmic and chloroplast triacylglycerol storage. *Progress in Lipid Research*, **80**, 101069.
Yang J. 2001. Hormonal changes in the grains of rice subjected to water stress during grain fifilling. *Plant Physiology*, **127**, 315–323.
Yen C L, Stone S J, Koliwad S, Harris C, Farese Jr R V. 2008. Thematic review series: Glycerolipids. DGAT enzymes and triacylglycerol biosynthesis. *Journal of Lipid Research*, **49**, 2283–2301.
Yu C W, Lin Y T, Li H M. 2020. Increased ratio of galactolipid MGDG: DGDG induces jasmonic acid overproduction and changes chloroplast shape. *The New Phytologist*, **228**, 1327–1335.
Yurchenko O P, Park S, Ilut D C, Inmon J J, Millhollon J C, Liechty Z, Page J T, Jenks M A, Chapman K D, Udall J A, Gore M A, Dyer J M. 2014. Genome-wide analysis of the omega-3 fatty acid desaturase gene family in *Gossypium*. *BMC Plant Biology*, **14**, 312.
Zegarlińska J, Piaścik M, Sikorski A F, Czogalla A. 2018. Phosphatidic acid — A simple phospholipid with multiple faces. *Acta Biochimica Polonica*, **65**, 163–171.
Zhang T, Hu Y, Jiang W, Fang L, Guan X, Chen J, Zhang J, Saski C A, Scheffler B E, Stelly D M, Hulse-Kemp A M, Wan Q, Liu B, Liu C, Wang S, Pan M, Wang Y, Wang D, Ye W, Chang L, *et al.* 2015. Sequencing of allotetraploid cotton (*Gossypium hirsutum* L. acc. TM-1) provides a resource for fiber improvement. *Nature Biotechnology*, **33**, 531–537.
Zhang Y, Zhu H, Zhang Q, Li M, Yan M, Wang R, Wang L, Welti R, Zhang W, Wang X. 2009. Phospholipase dalpha1 and phosphatidic acid regulate NADPH oxidase activity and production of reactive oxygen species in ABA-mediated stomatal closure in *Arabidopsis*. *The Plant Cell*, **21**, 2357–2377.
Zhu Y, Wang K, Wu C, Zhao Y, Yin X, Zhang B, Grierson D, Chen K, Xu C. 2019. Effect of ethylene on cell wall and lipid metabolism during alleviation of postharvest chilling injury in peach. *Cells*, **8**, 1612.
Zhu Y, Yuan G, Jia S, An G, Li W, Sun D, Liu J. 2022. Transcriptomic profiling of watermelon (*Citrullus lanatus*) provides insights into male flowers development. *Journal of Integrative Agriculture*, **21**, 407–421.

Executive Editor-in-Chief Xueyong Zhang
Managing Editor Ning Wang